

# Entanglement and thermodynamics after a quantum quench in integrable systems

Vincenzo Alba<sup>1</sup> and Pasquale Calabrese<sup>1</sup>

<sup>1</sup>*International School for Advanced Studies (SISSA), Via Bonomea 265, 34136, Trieste, Italy, INFN, Sezione di Trieste*

Entanglement and entropy are key concepts standing at the foundations of quantum and statistical mechanics. Recently, the study of quantum quenches revealed that these concepts are intricately intertwined. Although the unitary time evolution ensuing from a pure state maintains the system at zero entropy, local properties at long times are captured by a statistical ensemble with non zero thermodynamic entropy, which is the entanglement accumulated during the dynamics. Therefore, understanding the entanglement evolution unveils how thermodynamics emerges in isolated systems. Alas, an exact computation of the entanglement dynamics was available so far only for non-interacting systems, while it was deemed unfeasible for interacting ones. Here we show that the standard quasiparticle picture of the entanglement evolution, complemented with integrability-based knowledge of the steady state and its excitations, leads to a complete understanding of the entanglement dynamics in the space-time scaling limit. We thoroughly check our result for the paradigmatic Heisenberg chain.

Since the early days of quantum mechanics, understanding how statistical ensembles arise from the unitary time evolution of an isolated quantum system has been a fascinating question [1–7]. A widely accepted mechanism is that while the entire system remains in a pure state, the reduced density matrix of an arbitrary finite compact subsystem attains a long time limit that can be described by a statistical ensemble (see, e.g., Ref. [8]). In the last decade ground-breaking experiments with cold atoms [9–19] simulated with incredible precision the unitary time evolution of many-body quantum systems, reviving the interest in this topic. The simplest out-of-equilibrium protocol in which these ideas can be theoretically and experimentally tested is the quantum quench [20, 21]: A system is prepared in an initial state  $|\Psi_0\rangle$ , typically the ground state of a local Hamiltonian  $H_0$ , and it evolves with a many-body Hamiltonian  $H$ . At asymptotically long times, physical observables relax to stationary values, which for generic systems are described by the Gibbs (thermal) ensemble [3–7], whereas for *integrable* systems a Generalized Gibbs Ensemble (GGE) has to be used [8, 22–45].

Although these results suggest a spectacular compression of the amount of information needed to describe steady states, state-of-the-art numerical methods, such as the time-dependent Density Matrix Renormalization Group [46–49] (tDMRG), can only access the short-time dynamics. Physically, the origin of this conundrum is the fast growth of the entanglement entropy  $S \equiv -\text{Tr}_A \rho_A \ln \rho_A$ , with  $\rho_A$  being the reduced density matrix of an interval  $A$  of length  $\ell$  embedded in an infinite system. It is well-understood that  $S$  grows linearly with the time after the quench [50]. This implies an exponentially increasing amount of information manipulated during typical tDMRG simulations. Remarkably, the entanglement dynamics has been successfully observed in a very recent cold-atom experiment [19].

In this Letter, using a standard quasiparticle picture [50], we show that in integrable models the steady state and its low-lying excitations encode sufficient information to reconstruct the entanglement dynamics up to short times. According to the quasiparticle picture [50], the pre-quench initial state acts as a source of pairs of quasiparticle excitations. Let us first assume that there is only one type of quasiparticles identified

by their quasimomentum  $\lambda$ , and moving with velocity  $v(\lambda)$ . While quasiparticles created far apart from each other are incoherent, those emitted at the same point in space are entangled. As these propagate ballistically throughout the system, larger regions get entangled. At time  $t$ ,  $S(t)$  is proportional to the total number of quasiparticles that, emitted in pairs from the same point, reach one the subsystem  $A$  and the other its complement (see Fig. 1 (a)). Specifically, one obtains

$$S(t) \propto 2t \int_{2|v|t < \ell} d\lambda v(\lambda) f(\lambda) + \ell \int_{2|v|t > \ell} d\lambda f(\lambda), \quad (1)$$

where  $f(\lambda)$  depends on the production rate of quasiparticles. (1) holds in the space-time scaling limit  $t, \ell \rightarrow \infty$  at  $t/\ell$  fixed. When a maximum quasiparticle velocity  $v_M$  exists (e.g., due to the Lieb-Robinson bound [51]), for  $t \leq \ell/(2v_M)$ ,  $S$  grows linearly in time because the second term in (1) vanishes. In contrast, for  $t \gg \ell/(2v_M)$  the entanglement is extensive, i.e.,  $S \propto \ell$ . This light-cone spreading of entanglement has been confirmed analytically only in free models [52–57], numerically in several studies (see e.g. [58–60]), in the holographic framework [61–68], and in a recent experiment [19].

**Results.** In a generic interacting integrable model, there are different species of stable quasiparticles, corresponding to bound states of an arbitrary number of elementary excitations. Integrability implies that different types of quasiparticles must be treated independently. It is then natural to conjecture that

$$S(t) = \sum_n \left[ 2t \int_{2|v_n|t < \ell} d\lambda v_n(\lambda) s_n(\lambda) + \ell \int_{2|v_n|t > \ell} d\lambda s_n(\lambda) \right], \quad (2)$$

where the sum is over the types of particles  $n$ ,  $v_n(\lambda)$  is their velocity, and  $s_n(\lambda)$  their entropy. To give predictive power to (2), in the following we show how to determine  $v_n(\lambda)$  and  $s_n(\lambda)$  in the Bethe ansatz framework for integrable models.

The eigenstates of Bethe ansatz solvable models are in correspondence with a set of pseudomomenta (rapidities)  $\lambda$ . In the thermodynamic limit, these form a continuum. One then introduces the particle densities  $\rho_{n,p}(\lambda)$ , the hole (i.e., unoccupied rapidities) densities  $\rho_{n,h}(\lambda)$ , and the total densities  $\rho_{n,t}(\lambda) = \rho_{n,p}(\lambda) + \rho_{n,h}(\lambda)$ . Every set of den-

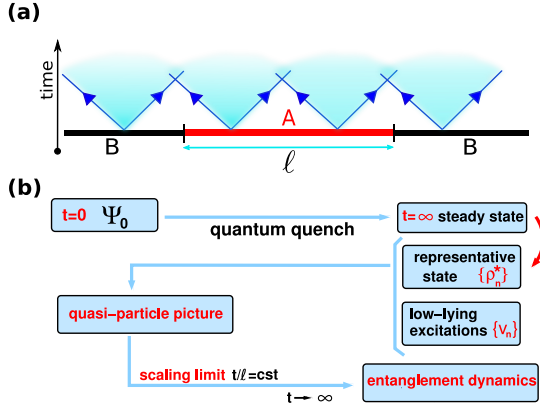


FIG. 1. Entanglement dynamics after a quantum quench: Theoretical scheme. (a) Quasiparticle picture. Full lines denote quasiparticles with maximum velocity emitted in the initial state. Shaded cones: Halo of slower quasiparticles. (b) Main steps to calculate the entanglement dynamics using Bethe ansatz and the quasiparticle picture.

sities identifies a thermodynamic “macro-state”. This corresponds to an exponentially large number of microscopic eigenstates, any of which can be used as a “representative” for the macro-state. The total number of representative microstates is  $e^{S_{YY}}$ , with  $S_{YY}$  the thermodynamic Yang-Yang entropy of the macrostate

$$\begin{aligned}
 S_{YY} &= s_{YY}L = L \sum_{n=1}^{\infty} \int d\lambda [\rho_{n,t}(\lambda) \ln \rho_{n,t}(\lambda) \\
 &\quad - \rho_{n,p}(\lambda) \ln \rho_{n,p}(\lambda) - \rho_{n,h}(\lambda) \ln \rho_{n,h}(\lambda)] \\
 &\equiv L \sum_{n=1}^{\infty} \int d\lambda s_{YY}^{(n)}[\rho_{n,p}, \rho_{n,h}](\lambda). \quad (3)
 \end{aligned}$$

Physically,  $S_{YY}$  corresponds to the total number of ways of assigning the quasimomentum label to the particles, similar to free-fermion models.

In the Bethe ansatz treatment of quantum quenches [69–71], local properties of the post-quench stationary state are described by a set of densities  $\rho_{n,p}^*(\lambda)$  and  $\rho_{n,h}^*(\lambda)$ . Calculating these densities is a challenging task that has been performed only in a few cases [72–84]. From the densities, the thermodynamic entropy of the stationary ensemble (3) is  $s_{YY}[\rho_{n,p}^*, \rho_{n,h}^*](\lambda)$ . Physically, this reflects a generalized microcanonical ensemble for quenches, in which all the microstates corresponding to the macrostate have the same probability.

We now present our predictions for the entanglement dynamics (Fig. 1 (b) gives a survey of our theoretical scheme). First, in the stationary state the density of thermodynamic entropy coincides with that of the entanglement entropy in (2), as it has been shown analytically for free models [52, 85, 86]. This implies that  $s_n(\lambda) = s_{YY}[\rho_{n,p}^*, \rho_{n,h}^*](\lambda)$ . Moreover, it is natural to identify the entangling quasiparticles in (2) with the low-lying excitations around the stationary state  $\rho^*$ . Their group velocities  $v_n$  depend on the stationary state, because

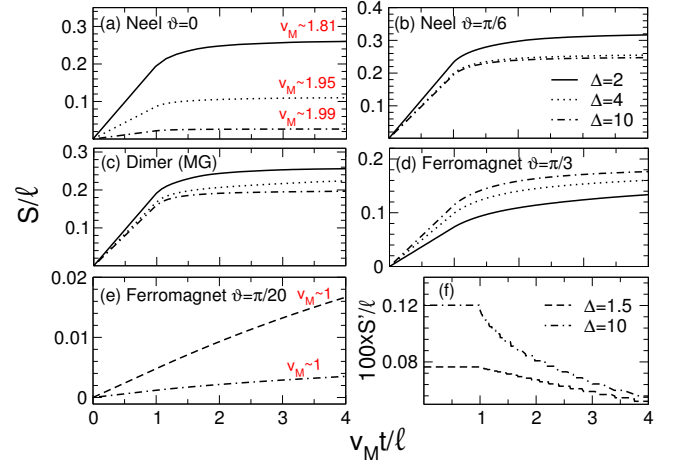


FIG. 2. Analytical predictions for the  $XXZ$  chain. Entanglement entropy per site  $S/\ell$  versus  $v_M t/\ell$ , with  $v_M$  the maximum velocity. Different panels correspond to the different initial states and different tilts to different  $\Delta$ . For  $\Delta \rightarrow \infty$ ,  $S \rightarrow 0$  for the Néel quench, whereas it saturates in the other cases. Note in (e) the substantial entanglement increase for  $v_M t/\ell > 1$ . Panel (f): The numerical derivative  $S'(v_M t/\ell) \times 100$  for the quench in (e).

the interactions induce a state-dependent dressing of the excitations. These velocities  $v_n$  can be calculated by Bethe ansatz techniques [87] (see Supplementary material).

To substantiate our idea we focus on the spin-1/2 anisotropic Heisenberg ( $XXZ$ ) chain, considering quenches from several low-entangled initial states, namely the tilted Néel state, the Majumdar-Ghosh (dimer) state, and the tilted ferromagnetic state (see the Methods paragraph). For these initial states the densities  $\rho_{n(h),p}^*$  are known analytically [74–76].

Fig. 2 summarizes the expected entanglement dynamics in the space-time scaling limit, plotting  $S/\ell$  versus  $v_M t/\ell$ . Interestingly,  $S/\ell$  is always smaller than  $\ln 2$ , i.e., the entropy

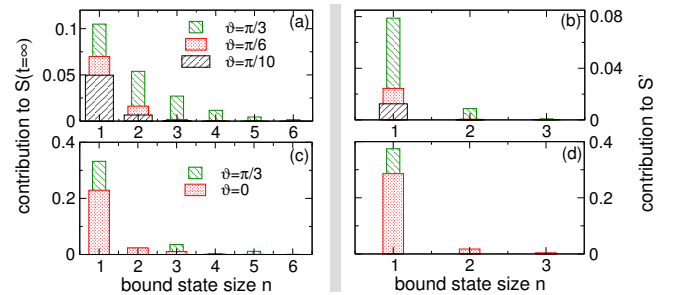


FIG. 3. Bound-state contributions to the entanglement dynamics. On the  $x$ -axis  $n$  is the bound-state size. (a)(b) Quench from the tilted ferromagnet. Panel (a): Bound-state contributions to steady-state entropy density (second term in (2)). Panel (b): Bound-state contributions to the slope of the entanglement growth for  $t < \ell/v_M$  (first term in (2)). Different histograms denote different tilting angles  $\vartheta$ . All the data are for  $\Delta = 2$ . (c)(d): same as in (a)(b) for the quench from the tilted Néel state.

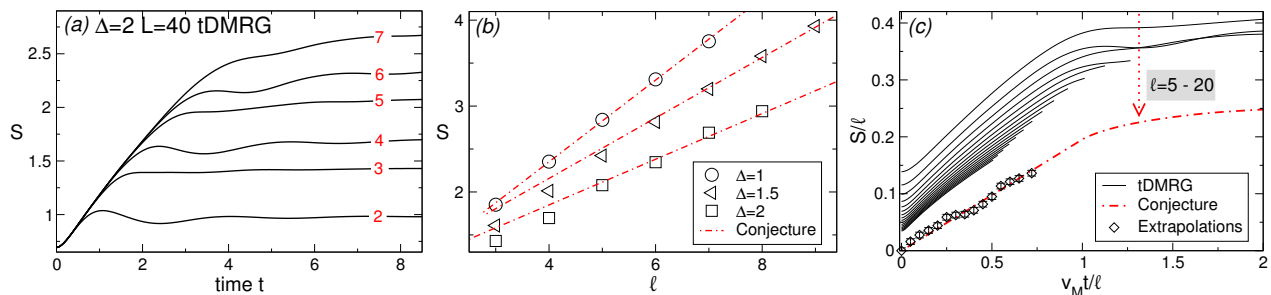


FIG. 4. Comparison with numerical simulations. Entanglement entropy dynamics after the quench from the Néel state in the  $XXZ$  chain. (a) tDMRG results for a chain with  $L = 40$  sites and  $\Delta = 2$ . Different curves correspond to different subsystem sizes  $\ell$  (accompanying numbers). (b) The entropy saturation values (tDMRG results at  $t \approx 8$ ) as a function of the block length  $\ell$ , for several  $\Delta$ . The dashed-dotted lines is the conjectured volume-law behavior  $S \propto s_{Y^*}^* \ell$  (cf. (3)). (c) The scaling limit:  $S/\ell$  plotted versus  $v_M t/\ell$ . The continuous curves are the tDMRG results for  $\ell = 5 - 20$ . The diamonds are numerical extrapolations to the thermodynamic limit. The dashed-dotted line is the conjecture (2).

of the maximally entangled state. For the Néel quench, since the Néel state becomes the ground state of (4) in the limit  $\Delta \rightarrow \infty$ ,  $S/\ell \approx \ln(\Delta)/\Delta^2$  vanishes, whereas it saturates for all the other quenches. For the Majumdar-Ghosh state one obtains  $S/\ell = -1/2 + \ln 2$  at  $\Delta \rightarrow \infty$ . For the tilted ferromagnet with  $\vartheta \rightarrow 0$  (Fig. 2 (e)),  $S/\ell$  is small at any  $\Delta$ , reflecting that the ferromagnet is an eigenstate of the  $XXZ$  chain. Surprisingly, the linear growth seems to extend for  $v_M t/\ell > 1$ . However,  $dS/dt$  (Fig. 2 (f)) is flat only for  $v_M t/\ell \leq 1$ , which signals true linear regime only for  $v_M t/\ell \leq 1$ . This peculiar behavior is due to the large entanglement contribution of the slow quasiparticles. In Fig. 3 we report the bound-state resolved contributions to the entanglement dynamics. Panel (a) and (c) focus on the steady state entropy (second term in (2)), while panels (b) and (d) show the bound-state contributions to the slope of the linear growth (first term in (2)). The contribution of the bound states, although never dominant, is crucial to ensure accurate predictions.

Fig. 4 (a) shows tDMRG results for  $S(t)$  for the quench from the symmetrized Néel state  $(|\uparrow\downarrow\uparrow \dots\rangle + |\downarrow\uparrow\downarrow \dots\rangle)/\sqrt{2}$ . The data are for the *open*  $XXZ$  chain, and subsystems starting from the chain boundary. The qualitative agreement with (2) is apparent. Fig. 4 (b) reports the steady-state entanglement entropy as a function  $\ell$  (data at  $t \approx 8$  in (a)). The volume-law  $S \propto \ell$  is visible. The dashed-dotted lines are fits to  $S \propto s_{Y^*}^* \ell$ , supporting the equivalence between entanglement and thermodynamic entropy. Fig. 4 (c) focuses on the full time dependence, plotting  $S/\ell$  versus  $v_M t/\ell$ . The dashed-dotted line is (2) with  $t \rightarrow t/2$ , due to the open boundary conditions [58]. Deviations from (2) due to the finite  $\ell$  are visible. The diamonds are numerical extrapolations to the thermodynamic limit. The agreement with (2) is perfect. Finally, we provide a more stringent check of (2), focusing on the linear entanglement growth. Fig. 5 shows infinite time-evolving block decimation (iTEBD) results in the thermodynamic limit for  $S'(v_M t)$ , with  $S'(x) \equiv dS(x)/dx$  taken from Ref. [88]. For all the quenches, the agreement with (2) (horizontal lines) is spectacular.

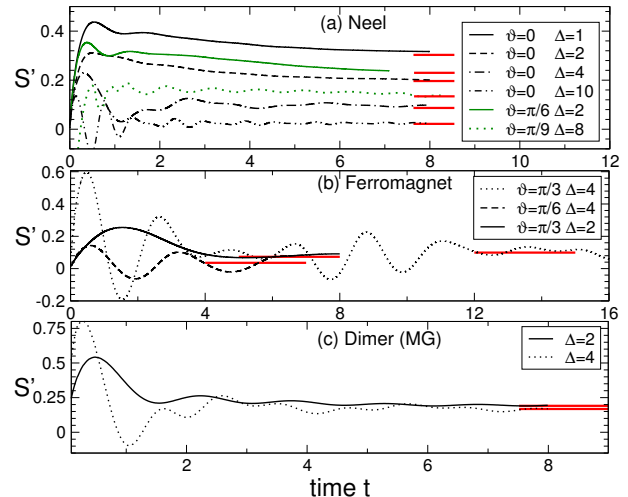


FIG. 5. Comparison with numerical simulations: The short-time regime. Derivative  $S'(v_M t)$  as a function of time. Different panels correspond to different initial states.  $\vartheta$  is the tilting angle. In each panel the different curves are iTEBD results for different  $\Delta$ . The horizontal lines are the conjecture (2).

**Conclusions.** The main result of this Letter is the analytical prediction in (2) for the time-dependent entanglement entropy after a generic quantum quench in an integrable model. We tested our conjecture for several quantum quenches in the  $XXZ$  spin chain, although we expect (2) to be more general. Further checks of (2) (e.g., for the Lieb-Liniger gas) are desirable. It would be also interesting to generalize (2) to quenches from inhomogeneous initial states, exploiting the recent analytical results [89–91]. Although we are not able yet to provide an *ab initio* derivation of (2), we find remarkable that it is possible to characterize analytically the dynamics of the entanglement entropy, while its equilibrium behavior is still an open challenge. Finally, we believe that (2) represents a deep conceptual breakthrough since it shows in a single compact formula the relation between entanglement and thermodynamic entropy for integrable models. An analogous description for non integrable systems, where quasiparticles

have finite lifetime or do not exist at all, could lead to a deeper understanding of thermalization [19].

**Methods.** The anisotropic spin-1/2 Heisenberg chain is defined by the Hamiltonian

$$H = \sum_{i=1}^L \left[ \frac{1}{2} (S_i^+ S_{i+1}^- + S_i^- S_{i+1}^+) + \Delta (S_i^z S_{i+1}^z - \frac{1}{4}) \right], \quad (4)$$

where  $S_i^\alpha$  are spin-1/2 operators, and  $\Delta$  is the anisotropy parameter. Here we considered as pre-quench initial states the tilted Néel state  $|\vartheta, \nearrow \searrow \dots\rangle \equiv e^{i\vartheta \sum_j S_j^y} |\uparrow \downarrow \dots\rangle$ , the Majumdar-Ghosh (dimer) state  $|MG\rangle \equiv ((|\uparrow \downarrow\rangle - |\downarrow \uparrow\rangle)/2)^{\otimes L/2}$ , and the tilted ferromagnetic state  $|\vartheta, \nearrow \nearrow\rangle \equiv e^{i\vartheta \sum_j S_j^y} |\uparrow \uparrow \dots\rangle$ . The Heisenberg spin chain is the prototype of all integrable models. Moreover, for all the initial states considered in this work the post-quench steady state can be characterized analytically, via the “macro-state” densities  $\rho_{p(h)}^*$ . Specifically, a set of recursive relations for these densities can be obtained (see Supplementary Material). The group velocities of the low-lying excitations around the steady state, i.e. the entangling quasiparticles, are obtained by solving numerically an infinite set of second type Fredholm integral equations (details are in the Supplementary Material).

The numerical data for the post-quench dynamics of the entanglement entropy presented in Fig. 4 were obtained using the standard tDMRG [46–49] in the framework of Matrix Product States (MPS). For the implementation we used the ITENSOR library (<http://itensor.org/>). The data presented in Figure 5 are obtained using the iTEBD method [92] and are a courtesy of Mario Collura.

**Acknowledgments.** The authors acknowledge support from the ERC under the Starting Grant 279391 EDEQS. This project has received funding from the European Union’s Horizon 2020 research and innovation programme under the Marie Skłodowska-Curie grant agreement No 702612 OEMBS. The iTEBD data presented in Fig. 5 are a courtesy of Mario Collura. We also thank Lorenzo Piroli and Eric Vernier for sharing their results before publication.

## REFERENCES

- 
- [1] von Neumann J. Beweis des Ergodensatzes und des H-Theorems. *Z Phys.* **57**, 30 (1929).
  - [2] Jensen RV and Shankar R. Statistical Behavior in Deterministic Quantum Systems with Few Degrees of Freedom. *Phys. Rev. Lett.* **54**, 1879 (1985).
  - [3] Deutsch JM, Quantum statistical mechanics in a closed system. *Phys. Rev. A* **43**, 2046 (1991).
  - [4] Srednicki M, Chaos and quantum thermalization. *Phys. Rev. E* **50**, 888 (1994).
  - [5] Rigol M, Dunjko V, and Olshanii M. Thermalization and its mechanism for generic isolated quantum systems. *Nature* **452**, 854 (2008).
  - [6] Rigol M and Srednicki M. Alternatives to Eigenstate Thermalization. *Phys. Rev. Lett.* **108**, 110601 (2012).
  - [7] D’Alessio L, Kafri Y, Polkovnikov A, and Rigol M. From Quantum Chaos and Eigenstate Thermalization to Statistical Mechanics and Thermodynamics. *Adv. Phys.* **65**, 239 (2016).
  - [8] Essler FHL and Fagotti M. Quench dynamics and relaxation in isolated integrable quantum spin chains. *J. Stat. Mech.* (2016) 064002.
  - [9] Kinoshita T, Wenger T, and Weiss, DS, A quantum Newton’s cradle. *Nature (London)* **440**, 900 (2008).
  - [10] Hofferberth S, Lesanovsky I, Fischer B, Schumm T, and Schiedmayer J, Non-equilibrium coherence dynamics in one-dimensional Bose gases. *Nature (London)* **449**, 324 (2007).
  - [11] Trotzky S, Chen Y-A, Flesch A, McCulloch IP, Schollwöck U, Eisert J, and Bloch I, Probing the relaxation towards equilibrium in an isolated strongly correlated one-dimensional Bose gas. *Nature Phys.* **8**, 325 (2012).
  - [12] Gring M, Kuhnert M, Langen T, Kitagawa T, Rauer B, Schreitl M, Mazets I, Smith DA, Demler E, and Schmiedmayer J. Relaxation and Prethermalization in an Isolated Quantum System. *Science* **337**, 6100 (2012).
  - [13] Cheneau M, Barmettler P, Poletti D, Endres M, Schauß P, Fukuhara T, Gross C, Bloch I, Kollath C, and Kuhr S. Light-cone-like spreading of correlations in a quantum many-body system. *Nature* **481**, 484 (2012).
  - [14] Langen T, Geiger R, Kuhnert M, Rauer B, and Schmiedmayer J, Local emergence of thermal correlations in an isolated quantum many-body system. *Nature Phys.* **9**, 640 (2013).
  - [15] Meinert F, Mark MJ, Kirilov E, Lauber K, Weinmann P, Daley AJ, and Nagerl H-C. Quantum Quench in an Atomic One-Dimensional Ising Chain. *Phys. Rev. Lett.* **111**, 053003 (2013).
  - [16] Fukuhara T, Kantian A, Endres M, Cheneau M, Schauß P, Hild S, Gross C, Schollwöck U, Giamarchi T, Bloch I, and Kuhr S. Quantum dynamics of a mobile spin impurity. *Nature Phys.* **9**, 235 (2013).
  - [17] Langen T, Erne S, Geiger R, Rauer B, Schweigier T, Kuhnert M, Rohringer W, Mazets IE, Gasenzer T, Schmiedmayer J. Experimental observation of a generalized Gibbs ensemble. *Science* **348**, 6231 (2015).
  - [18] Islam R, Ma R, Preiss PM, Tai ME, Lukin A, Rispoli M, and Greiner M. Measuring entanglement entropy in a quantum many-body system. *Nature* **528**, 77 (2015).
  - [19] Kaufman AM, Tai ME, Lukin A, Rispoli M, Schittko R, Preiss PM, and Greiner M. Quantum thermalization through entanglement in an isolated many-body system. *Science* **353**, 794 (2016).
  - [20] Calabrese P and Cardy J. Time Dependence of Correlation Functions Following a Quantum Quench. *Phys. Rev. Lett.* **96**, 136801 (2006).
  - [21] Polkovnikov A, Sengupta K, Silva A, and Vengalattore M, *Colloquium*: Nonequilibrium dynamics of closed interacting quantum systems. *Rev. Mod. Phys.* **83**, 863 (2011).
  - [22] Rigol M, Dunjko V, Yurovsky V, and Olshanii M. Relaxation in a Completely Integrable Many-Body Quantum System: An *Ab Initio* Study of the Dynamics of the Highly Excited States of 1D Lattice Hard-Core Bosons. *Phys. Rev. Lett.* **98**, 050405 (2007).
  - [23] Cazalilla MA. Effect of Suddenly Turning on Interactions in the Luttinger Model. *Phys. Rev. Lett.* **97**, 156403 (2006).
  - [24] Barthel T and Schollwöck U. Dephasing and the Steady State in Quantum Many-Particle Systems. *Phys. Rev. Lett.* **100**, 100601 (2008).

- [25] Cramer M, Dawson CM, Eisert J, and Osborne TJ. Exact Relaxation in a Class of Nonequilibrium Quantum Lattice Systems. *Phys. Rev. Lett.* **100**, 030602 (2008).
- [26] Cramer M and Eisert J. A quantum central limit theorem for non-equilibrium systems: exact local relaxation of correlated states. *New J. Phys.* **12**, 055020 (2010).
- [27] Calabrese P, Essler FHL, and Fagotti M. Quantum Quench in the Transverse-Field Ising Chain. *Phys. Rev. Lett.* **106**, 227203 (2011).
- [28] Cazalilla MA, Iucci A, and Chung M-C. Thermalization and quantum correlations in exactly solvable models. *Phys. Rev. E* **85**, 011133 (2012).
- [29] Calabrese P, Essler FHL, and Fagotti M. Quantum Quench in the Transverse Field Ising Chain II: Stationary State Properties. *J. Stat. Mech.* (2012) P07022.
- [30] Sotiriadis S, Fioretto D, and Mussardo G. Zamolodchikov-Faddeev Algebra and Quantum Quenches in Integrable Field Theories. *J. Stat. Mech.* (2012) P02017.
- [31] Collura M, Sotiriadis S, and Calabrese P. Equilibration of a Tonks-Girardeau Gas Following a Trap Release. *Phys. Rev. Lett.* **110**, 245301 (2013).
- [32] Collura M, Sotiriadis S, and Calabrese P. Quench dynamics of a Tonks-Girardeau gas released from a harmonic trap. *J. Stat. Mech.* P09025 (2013).
- [33] Fagotti M and Essler FHL. Stationary behaviour of observables after a quantum quench in the spin-1/2 Heisenberg  $XXZ$  chain. *J. Stat. Mech.* (2013) P07012.
- [34] Kormos M, Collura M, and Calabrese P. Analytic results for a quantum quench from free to hard-core one-dimensional bosons. *Phys. Rev. A* **89**, 013609 (2014).
- [35] Sotiriadis S and Calabrese P. Validity of the GGE for quantum quenches from interacting to noninteracting models. *J. Stat. Mech.* (2014) P07024.
- [36] Ilievski E, De Nardis J, Wouters B, Caux J-S, Essler FHL, and Prosen T. Complete Generalized Gibbs Ensembles in an Interacting Theory. *Phys. Rev. Lett.* **115**, 157201 (2015).
- [37] Alba V. Simulating the Generalized Gibbs Ensemble (GGE): a Hilbert space Monte Carlo approach. arXiv:1507.06994.
- [38] Essler FHL, Mussardo G, and Panfil M. Generalized Gibbs ensembles for quantum field theories. *Phys. Rev. A* **91**, 051602 (2015).
- [39] Cardy J. Quantum quenches to a critical point in one dimension: some further results. *J. Stat. Mech.* (2016) 023103.
- [40] Sotiriadis S. Memory-preserving equilibration after a quantum quench in a 1d critical model. *Phys. Rev. A* **94**, 031605 (2016).
- [41] Bastianello A and Sotiriadis S. Quasi locality of the GGE in interacting-to-free quenches in relativistic field theories. arXiv:1608.00924.
- [42] Vernier E, and Cubero AC. Quasilocal charges and the complete GGE for field theories with non diagonal scattering. arXiv:1609.03220.
- [43] Vidmar L and Rigol M. Generalized Gibbs ensemble in integrable lattice models. *J. Stat. Mech.* 064007 (2016).
- [44] Gogolin C and Eisert J. Equilibration, thermalisation, and the emergence of statistical mechanics in closed quantum systems. *Rep. Prog. Phys.* **79**, 056001 (2016).
- [45] Calabrese P, Essler FHL, and Mussardo G. Introduction to “Quantum Integrability in Out of Equilibrium Systems” (2016) 064001.
- [46] White SR and Feiguin AE. Real-Time Evolution Using the Density Matrix Renormalization Group. *Phys. Rev. Lett.* **93**, 076401 (2004).
- [47] Daley AJ, Kollath C, Schollwöck U, and Vidal G. Time-dependent density-matrix renormalization-group using adaptive effective Hilbert spaces. *J. Stat. Mech.* (2004) P04005.
- [48] Schollwöck U. The density-matrix renormalization group. *Rev. Mod. Phys.* **77**, 259 (2005).
- [49] Schollwöck U. The density-matrix renormalization group in the age of matrix product states. *Annals of Physics* **326**, 96 (2011).
- [50] Calabrese P and Cardy J. Evolution of Entanglement Entropy in One-Dimensional Systems. *J. Stat. Mech.* (2005) P04010.
- [51] Lieb EH and Robinson DW. The finite group velocity of quantum spin systems. *Commun. Math. Phys.* **28**, 251 (1972).
- [52] Fagotti M and Calabrese P. Evolution of entanglement entropy following a quantum quench: Analytic results for the XY chain in a transverse magnetic field. *Phys. Rev. A* **78**, 010306 (2008).
- [53] Eisler V and Peschel I. Entanglement in a periodic quench. *Ann. Phys. (Berlin)* **17**, 410 (2008).
- [54] Ghasemi Nezhadhighi M, and Rajabpour MA. Entanglement dynamics in short and long-range harmonic oscillators. *Phys. Rev. B* **90**, 205438 (2014).
- [55] Coser A, Tonni E, and Calabrese P. Entanglement negativity after a global quantum quench. *J. Stat. Mech.* P12017 (2014).
- [56] Cotler JS, Hertzberg MP, Mezei M, and Mueller MT. Entanglement Growth after a Global Quench in Free Scalar Field Theory. *JHEP* **11** (2016) 166.
- [57] Buyskikh AS, Fagotti M, Schachenmayer J, Essler FHL, and Daley AJ. Entanglement growth and correlation spreading with variable-range interactions in spin and fermionic tunneling models. *Phys. Rev. A* **93**, 053620 (2016).
- [58] De Chiara G, Montangero S, Calabrese P, and Fazio R. Entanglement Entropy dynamics in Heisenberg chains. *J. Stat. Mech.* P03001 (2006).
- [59] Läuchli AM and Kollath C. Spreading of correlations and entanglement after a quench in the one-dimensional Bose-Hubbard model. *J. Stat. Mech.* P05018 (2008).
- [60] Kim H and Huse, DA. Ballistic Spreading of Entanglement in a Diffusive Nonintegrable System. *Phys. Rev. Lett.* **111**, 127205 (2013).
- [61] Hubeny VE, Rangamani M, and Takayanagi T. A Covariant holographic entanglement entropy proposal. *JHEP* **0707**, 062 (2007);
- [62] Abajo-Arrastia J, Aparicio J, and Lopez E. Holographic Evolution of Entanglement Entropy. *JHEP* **1011** 149 (2010).
- [63] Albash T and Johnson CV. Evolution of Holographic Entanglement Entropy after Thermal and Electromagnetic Quenches. *New J. Phys.* **13**, 045017 (2011).
- [64] Allais A and Tonni E. Holographic evolution of the mutual information. *JHEP* **1201** 102 (2012).
- [65] Callan R, He J-Y, and Headrick M. Strong subadditivity and the covariant holographic entanglement entropy formula. *JHEP* **1206**, 081 (2012).
- [66] Liu H and Suh SJ. Entanglement Tsunami: Universal Scaling in Holographic Thermalization. *Phys. Rev. Lett.* **112**, 011601 (2014).
- [67] Balasubramanian V, Bernamonti A, Copland N, Craps B, and Galli F. Thermalization of mutual and tripartite information in strongly coupled two dimensional conformal field theories. *Phys. Rev. D* **84**, 105017 (2011).
- [68] Liu H and Suh SJ. Entanglement growth during thermalization in holographic systems. *Phys. Rev. D* **89**, 066012 (2014).
- [69] Caux J-S, and Essler FHL. Time evolution of local observables after quenching to an integrable model. *Phys. Rev. Lett.* **110**, 257203 (2013).
- [70] Caux J-S. The Quench Action. *J. Stat. Mech.* (2016) 064006.

- [71] Ilievski E, Quinn E, De Nardis J, and Brockmann M. String-charge duality in integrable lattice models. *J. Stat. Mech.* (2016) 063101.
- [72] Bertini B, Schuricht D, and Essler FHL. Quantum quench in the sine-Gordon model. *J. Stat. Mech.* (2014) P10035.
- [73] De Nardis J, Wouters B, Brockmann M, and Caux J-S. Solution for an interaction quench in the Lieb-Liniger Bose gas. *Phys. Rev. A* **89**, 033601 (2014).
- [74] Wouters B, Brockmann M, De Nardis J, Fioretto D, Rigol M, and Caux, J-S. Quenching the Anisotropic Heisenberg Chain: Exact Solution and Generalized Gibbs Ensemble Predictions. *Phys. Rev. Lett.* **113**, 117202 (2014).
- [75] Pozsgay B, Mestyán M, Werner MA, Kormos M, Zaránd G, and Takács G. Correlations after Quantum Quenches in the XXZ Spin Chain: Failure of the Generalized Gibbs Ensemble. *Phys. Rev. Lett.* **113**, 117203 (2014).
- [76] Piroli L, Vernier E, and Calabrese P. Exact steady states for quantum quenches in integrable Heisenberg spin chains. *Phys. Rev. B* **94**, 054313 (2016).
- [77] Brockmann M, Wouters B, Fioretto D, De Nardis J, Vlijm R, and Caux J-S. Quench action approach for releasing the Neel state into the spin-1/2 XXZ chain. *J. Stat. Mech.* (2014) P12009.
- [78] Mestyán M, Pozsgay B, Takács G, and Werner MA. Quenching the XXZ spin chain: quench action approach versus generalized Gibbs ensemble. *J. Stat. Mech.* (2015) P04001.
- [79] Bucciantini L. Stationary State After a Quench to the Lieb-Liniger from Rotating BECs. *J. Stat. Phys.* **164**, 621 (2016).
- [80] Bertini B, Piroli L, and Calabrese P. Quantum quenches in the sinh-Gordon model: steady state and one-point correlation functions. *J. Stat. Mech.* (2016) 063102.
- [81] Alba V and Calabrese P. The quench action approach in finite integrable spin chains. *J. Stat. Mech.* (2016), 043105.
- [82] Piroli L, Calabrese P, and Essler FHL. Multiparticle Bound-State Formation following a Quantum Quench to the One-Dimensional Bose Gas with Attractive Interactions. *Phys. Rev. Lett.* **116**, 070408 (2016).
- [83] Piroli L, Calabrese P, and Essler FHL. Quantum quenches to the attractive one-dimensional Bose gas: exact results. *SciPost Phys.* 1(1), 001 (2016).
- [84] Piroli L, Vernier E, Calabrese P, and Rigol M. Correlations and diagonal entropy after quantum quenches in XXZ chains. *Phys. Rev. B* **95**, 054308 (2017).
- [85] Collura M, Kormos M, and Calabrese P. Stationary entanglement entropies following an interaction quench in 1D Bose gas. *J. Stat. Mech.* P01009 (2014).
- [86] Kormos M, Bucciantini L, and Calabrese P. Stationary entropies after a quench from excited states in the Ising chain. *EPL* **107**, 40002 (2014).
- [87] Bonnes L, Essler FHL, and Läuchli AM. Light-Cone Dynamics After Quantum Quenches in Spin Chains. *Phys. Rev. Lett.* **113**, 187203 (2014).
- [88] Fagotti M, Collura M, Essler FHL, and Calabrese P. Relaxation after quantum quenches in the spin-1/2 Heisenberg XXZ chain. *Phys. Rev. B* **89**, 125101 (2014).
- [89] Castro-Alvaredo OA, Doyon B, and Yoshimura T. Emergent hydrodynamics in integrable quantum systems out of equilibrium. *Phys. Rev. X* **6**, 041065 (2016).
- [90] Bertini B, Collura M, De Nardis J, and Fagotti M. Transport in out-of-equilibrium XXZ chains: exact profiles of charges and currents. *Phys. Rev. Lett.* **117**, 207201 (2016).
- [91] Dubail J, Stéphan J-M, Viti J, and Calabrese P. Conformal Field Theory for Inhomogeneous One-dimensional Quantum Systems: the Example of Non-Interacting Fermi Gases. *SciPost Phys.* **2**, 002 (2017).
- [92] Vidal G. Classical Simulation of Infinite-Size Quantum Lattice Systems in One Spatial Dimension. *Phys. Rev. Lett.* **98**, 070201 (2007).
- [93] Takahashi M., *Thermodynamics of one-dimensional solvable models*, Cambridge University Press, Cambridge, 1999.
- [94] Yang CN and Yang CP. Thermodynamics of a One-Dimensional System of Bosons with Repulsive Delta Function Interaction. *J. Math. Phys.* **10**, 1115 (1969).
- [95] De Nardis J, Piroli L, and Caux J-S. Relaxation dynamics of local observables in integrable systems. *J. Phys. A* **48**, 43FT01 (2015).
- [96] Calabrese P and Cardy J. Quantum quenches in extended systems. *J. Stat. Mech.* (2007) P06008.
- [97] Gambassi A and Calabrese P. Quantum quenches as classical critical films. *EPL* **95** (2011) 66007.
- [98] Delfino G, Quantum quenches with integrable pre-quench dynamics. *J. Phys. A* **47** (2014) 402001.
- [99] Collura M, Calabrese P, and Essler FHL. Quantum quench within the gapless phase of the spin-1/2 Heisenberg  $XXZ$  spin-chain. *Phys. Rev. B* **92**, 125131 (2015).
- [100] Calabrese P and Cardy J. Quantum quenches in 1+1 dimensional conformal field theories *J. Stat. Mech.* (2016) 064003.
- [101] Barbiero L and Dell'Anna L. Spreading of correlations in quenched repulsive and attractive one dimensional lattice system. arXiv:1609.07387.
- [102] Kormos M, Collura M, Takács G, and Calabrese P. Real time confinement following a quantum quench to a non-integrable model. arXiv:1604.03571.
- [103] Bertini B, Essler FHL, Groha S, and Robinson N. Thermalization and light cones in a model with weak integrability breaking. *Phys. Rev. B* **94**, 245117 (2016).
- [104] Chiocchetta A, Tavora M, Gambassi A, and Mitra A. Short-time universal scaling and light-cone dynamics after a quench in an isolated quantum system in  $d$  spatial dimensions. *Phys. Rev. B* **94**, 134311 (2016).
- [105] Asplund CT and Bernamonti A. Mutual information after a local quench in conformal field theory, *Phys. Rev. D* **89**, 066015 (2014).
- [106] Leichenauer S and Moosa M. Entanglement Tsunami in (1+1)-Dimensions, *Phys. Rev. D* **92**, 126004 (2015).
- [107] Asplund CT, Bernamonti A, Galli F, and Hartmann T. Entanglement Scrambling in 2d Conformal Field Theory, *JHEP* **09**, 110 (2015).
- [108] Fagotti M and Calabrese P. Entanglement entropy of two disjoint blocks in XY chains. *J. Stat. Mech.* (2010) P04016.

## SUPPLEMENTAL MATERIAL

- In this Supplementary material we provide some details on:
- (1) The Bethe ansatz solution of the  $XXZ$  chain.
  - (2) The Bethe ansatz treatment of the post-quench steady state.
  - (3) The calculation of the group velocities of the low-lying excitations around the steady state.
  - (4) The entanglement and the mutual information of two disjoint intervals.

## BETHE ANSATZ SOLUTION OF THE $XXZ$ CHAIN

In the Bethe ansatz [93] solution of the  $XXZ$  chain, the eigenstates of (4) in the sector with  $M$  down spins (particles) are in correspondence with a set of rapidities  $\lambda_j$ . These are obtained by solving the Bethe equations [93]

$$\left[ \frac{\sin(\lambda_j + i\frac{\eta}{2})}{\sin(\lambda_j - i\frac{\eta}{2})} \right]^L = - \prod_{k=1}^M \frac{\sin(\lambda_j - \lambda_k + i\eta)}{\sin(\lambda_j - \lambda_k - i\eta)}, \quad (5)$$

where  $\eta \equiv \text{arccosh}(\Delta)$ .

In the thermodynamic limit the solutions of the Bethe equations (5) form string patterns in the complex plane. The rapidities forming a  $n$ -string are parametrized as

$$\lambda_{n,\gamma}^j = \lambda_{n,\gamma} + i\frac{\eta}{2}(n+1-2j) + \delta_{n,\gamma}^j, \quad (6)$$

where  $j = 1, \dots, n$  labels the different string components,  $\lambda_{n,\gamma}$  is the ‘‘string center’’, and  $\delta_{n,\gamma}^j$  are the so-called string deviations. Typically, i.e., for the majority of the eigenstates of (4), one has  $\delta_{n,\gamma}^j = \mathcal{O}(e^{-L})$ , implying that the string deviations can be neglected [93] (string hypothesis). Physically,  $n$ -strings correspond to bound states of  $n$  down spins. The string centers  $\lambda_{n,\gamma}$  are solutions of the Bethe-Gaudin-Takahashi (BGT) equations [93]

$$L\theta_n(\lambda_{n,\alpha}) = 2\pi I_{n,\alpha} + \sum_{(n,\alpha) \neq (m,\beta)} \Theta_{n,m}(\lambda_{n,\alpha} - \lambda_{m,\beta}). \quad (7)$$

For  $\Delta > 1$ , one has  $\lambda_{n,\gamma} \in [-\pi/2, \pi/2)$ . Here we define  $\theta_n(\lambda) \equiv 2 \arctan[\tan(\lambda)/\tanh(n\eta/2)]$ . The scattering phases  $\Theta_{n,m}(\lambda)$  are defined as

$$\Theta_{n,m}(\lambda) \equiv (1 - \delta_{n,m})\theta_{|n-m|}(\lambda) + 2\theta_{|n-m|+2}(\lambda) + \dots + \theta_{n+m-2}(\lambda) + \theta_{n+m}(\lambda). \quad (8)$$

Each different choice of the so-called BGT quantum numbers  $I_{n,\alpha} \in \frac{1}{2}\mathbb{Z}$  identifies a different set of solutions of (7), and, in turn, a different eigenstate of (4). The corresponding eigenstate energy  $E$  and total momentum  $P$  are obtained by summing over all the BGT rapidities [93] as  $E = \sum_{n,\alpha} \epsilon_n(\lambda_{n,\alpha})$ , and  $P = \sum_{n,\alpha} z_n(\lambda_{n,\alpha})$  with

$$\epsilon_n(\lambda) \equiv -\frac{\sinh(\eta) \sinh(n\eta)}{\cosh(n\eta) - \cos(2\lambda)}, \quad z_n(\lambda_{n,\alpha}) = \frac{2\pi I_{n,\alpha}}{L}. \quad (9)$$

Note that  $P$  depends only on the  $I_{n,\alpha}$ .

## THE STEADY STATE: BETHE ANSATZ TREATMENT

Here we provide some details on how to derive the steady-state densities  $\rho_{n,p}^*, \rho_{n,h}^*$  in Bethe ansatz. First, the root densities  $\rho_{n,p}$  are defined as [94]

$$\rho_{n,p}(\lambda) \equiv \lim_{L \rightarrow \infty} \frac{1}{L(\lambda_{n,\alpha+1} - \lambda_{n,\alpha})}. \quad (10)$$

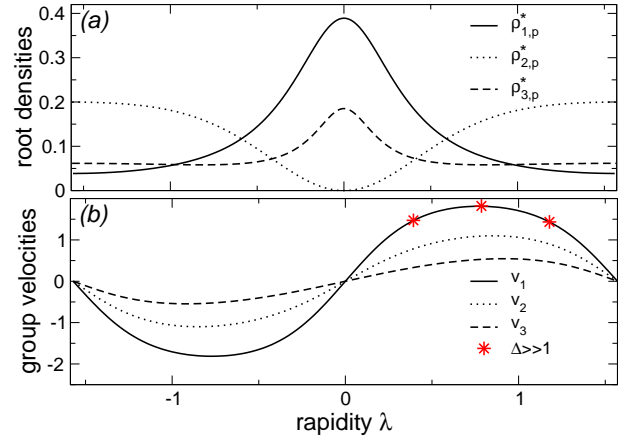


FIG. 6. The post-quench steady state and the low-lying excitations around it. Results for the quench from the Néel state in the  $XXZ$  chain with  $\Delta = 2$ . (a) The macro-state densities  $\rho_{n,p}^*$  characterizing the steady state. The first three particle densities  $\rho_n^*(\lambda)$  plotted against the rapidity  $\lambda$ . (b) Group velocities of the low-lying excitations around the steady-state macro state, as a function of  $\lambda$ . Note that  $v_n(-\lambda) = -v_n(\lambda)$ . The star symbols are the results for  $\Delta \gg 1$ .

Instead of working with the hole densities  $\rho_{n,h}$ , it is convenient to define  $\eta_n = \rho_{n,h}/\rho_{n,p}$ . For all the initial states considered in this work the corresponding steady-state densities  $\rho_{n,h}^*, \eta_n^*$  obey the recursive relations [71, 77]

$$\eta_n^*(\lambda) = \frac{\eta_{n-1}^*(\lambda + i\frac{\eta}{2})\eta_{n-1}^*(\lambda - i\frac{\eta}{2})}{1 + \eta_{n-2}^*(\lambda)} - 1, \quad (11)$$

$$\rho_{n,h}^*(\lambda) = \rho_{n,t}^*(\lambda + i\frac{\eta}{2}) + \rho_{n,t}^*(\lambda) - \rho_{n-1,h}^*(\lambda), \quad (12)$$

with  $\eta_0^* = 0$  and  $\rho_{0,h}^* = 0$ . In (11) and (12) the initial conditions  $\rho_{1,h}^*$  and  $\eta_1^*$  encode the information about the pre-quench initial state. For all the quenches considered in this work, this initial conditions are known analytically. For instance, for the quench from the Néel state one has [77]

$$\eta_1^* = \frac{2[2 \cosh(\eta) + 2 \cosh(3\eta) - 3 \cos(2\lambda) \sin^2(\lambda)]}{[\cosh(\eta) - \cos(2\lambda)][\cosh(4\eta) - \cos(4\lambda)]} \quad (13)$$

$$\rho_{1,h}^* = \frac{\theta_1'(\lambda)}{2\pi} \left( 1 - \frac{4 \cosh^2(\eta)}{[\theta_1'(\lambda) \sin(2\lambda)]^2 + 4 \cosh^2(\eta)} \right),$$

where  $\theta_1'(\lambda) \equiv d\theta_1(\lambda)/d\lambda$  (with  $\theta_1(\lambda)$  as defined in (8)). For the dimer state  $\rho_{1,p}^*$  and  $\eta_1^*$  have been calculated in [78] while for the tilted Néel and the tilted ferromagnet they have been derived recently [76, 84]. Figure 6 (a) shows  $\rho_{n,p}^*$  for  $n = 1, 2, 3$  for the quench from the Néel state in the  $XXZ$  chain with  $\Delta = 2$ .

## GROUP VELOCITIES OF THE ENTANGLING QUASIPARTICLES

Here we detail the calculation of the group velocities of the entangling quasiparticles, which explain the linear entanglement growth after the quench. The low-lying excitations

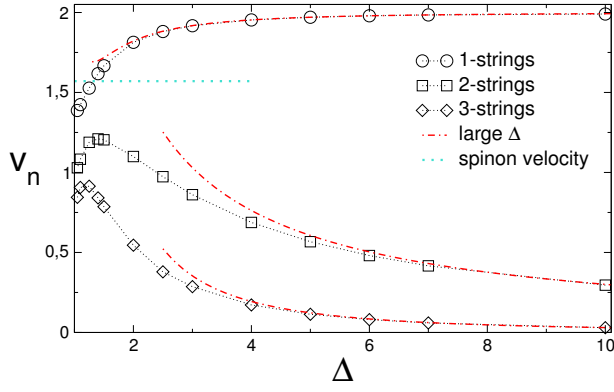


FIG. 7. Group velocities of the low-lying excitations around the steady state after the quench from the Néel state in the  $XXZ$  chain. The maximum velocity in each string sector (different symbols in the Fig.) is plotted against the anisotropy  $\Delta$ . The dash-dotted lines are the analytical results (18) in the large  $\Delta$  limit. The horizontal dotted line is the (low-energy) spin wave velocity  $v_{sw} = \pi/2$  at  $\Delta = 1$ .

around the post-quench steady state can be constructed as particle-hole excitations over the corresponding macro-state. Notice that it has been verified in Ref. [95] that the low-lying excitations around the stationary state can be used to reconstruct “back in time” the post-quench out-of-equilibrium dynamics of local observables. First, one can imagine choosing among the eigenstates of (4) a representative of the macro-state, identified by some BGT quantum numbers  $I_{n,\alpha}^*$ . Then, a particle-hole excitation, in each  $n$ -string sector, is obtained as  $I_{n,h}^* \rightarrow I_{n,p}$ , where  $I_{n,p}(I_{n,h}^*)$  is the BGT number of the added particle (hole). Since the  $XXZ$  chain is interacting, this local change in quantum numbers affects *all* the new rapidities. The excess energy of the particle-hole excitation is

$$\delta E_n = e_n(\lambda_{n,p}^*) - e_n(\lambda_{n,h}^*). \quad (14)$$

Remarkably, apart from the dressing of the “single-particle” energy  $e(\lambda)$  (see below for its calculation), (14) is the same as for free models. The change in the total momentum is obtained from (9) as

$$\delta P = z_n(\lambda_{n,p}^*) - z_n(\lambda_{n,h}^*). \quad (15)$$

Finally, the group velocity of the particle-hole excitations is by definition

$$v_n(\lambda) \equiv \frac{\partial e_n}{\partial z_n} = \frac{e'_n(\lambda)}{2\pi\rho_{n,t}^*(1 + \eta_n^*(\lambda))}. \quad (16)$$

Here we used that [93]  $dz_n(\lambda)/d\lambda = 2\pi\rho_{n,t}^*$ , with  $\rho_{n,t}^* \equiv \rho_{n,p}^*(1 + \eta_n^*)$ , and we defined  $e'_n(\lambda)$  as the derivative of  $e(\lambda)$ . Importantly,  $e'_n(\lambda)$  is determined by an infinite system of Fredholm integral equations of the second kind as

$$e'_n(\lambda) + \frac{1}{2\pi} \sum_{m=1}^{\infty} \int d\mu e'_m(\mu) \frac{\Theta'_{m,n}(\mu - \lambda)}{1 + \eta_m^*(\mu)} = \epsilon'_n(\lambda), \quad (17)$$

where  $\Theta'_{n,m}(\lambda) \equiv d\Theta_{n,m}(\lambda)/d\lambda$  and  $\epsilon'_n(\lambda) \equiv de_n(\lambda)/d\lambda$  (cf. also (8) and (9)). The solutions of (17) can be obtained numerically very effectively after truncating the system considering  $n \leq n_{max}$ . We should mention that the method outlined above has been used to study transport properties in the  $XXZ$  chain starting from inhomogeneous initial conditions [89, 90], and the spreading of correlations after quantum quenches [87] (see also [20, 96–104]).

Importantly, in the limit  $\Delta \rightarrow \infty$  the solution of (17), and the group velocities (16) can be obtained *analytically* as a power series in  $z \equiv e^{-\eta} \approx 1/(2\Delta)$ . For instance, for the quench from the Néel state one obtains

$$\begin{aligned} v_1(\lambda) &= 2 \sin(2\lambda) + z^2 [\sin(2\lambda) + 4 \cos(4\lambda) \sin(2\lambda)] \\ &\quad + z^3 [2 \cos(2\lambda) \sin(2\lambda)] - z^4 [2 \cos(4\lambda) \sin(2\lambda) \\ &\quad - \sin(2\lambda) - 4 \cos(8\lambda) \sin(2\lambda)] + \mathcal{O}(z^5) \\ v_2(\lambda) &= 6z \sin(2\lambda) + \mathcal{O}(z^3) \\ v_3(\lambda) &= 12z^2 \sin(2\lambda) + \mathcal{O}(z^3). \end{aligned} \quad (18)$$

A similar result can be obtained for the Majumdar-Ghosh state as

$$\begin{aligned} v_1(\lambda) &= 2 \sin(2\lambda) + 4z^2 \cos(4\lambda) \sin(2\lambda) \\ &\quad + z^3 [8 \cos(2\lambda) \sin(2\lambda) + 4 \sin(2\lambda)] \\ &\quad + z^4 [6 \sin(2\lambda) - 4 \cos(2\lambda) \sin(2\lambda) + \\ &\quad - 8 \cos(4\lambda) \sin(2\lambda) + 4 \cos(8\lambda) \sin(2\lambda)] + \mathcal{O}(z^5) \\ v_2(\lambda) &= 4z \sin(2\lambda) \\ &\quad + z^2 [4 \sin(2\lambda) + 4 \cos(2\lambda) \sin(2\lambda)] \\ &\quad + z^3 [4 \cos(4\lambda) \sin(2\lambda) - 6 \sin(2\lambda)] \\ &\quad + z^4 [4 \cos(6\lambda) \sin(2\lambda) - 28 \sin(2\lambda) \\ &\quad - 32 \cos(2\lambda) \sin(2\lambda)] + \mathcal{O}(z^5) \\ v_3(\lambda) &= 12z^2 \sin(2\lambda) + \mathcal{O}(z^3). \end{aligned} \quad (19)$$

As an example of calculation of group velocities we plot in Figure 6 (b)  $v_n^*(\lambda)$  for  $n = 1, 2, 3$  for the quench from the Néel state in the  $XXZ$  chain with  $\Delta = 2$ . In the figure,  $v_n$  are plotted versus the rapidity  $\lambda$ . The star symbols are the perturbative results (18) in the large  $\Delta$  limit. Moreover, in Figure 7 we plot the maximum group velocity in each string sector as a function of  $\Delta$ . The dash-dotted lines are the analytical results (18) in the limit  $\Delta \rightarrow \infty$ . Note that in the limit  $\Delta \rightarrow \infty$  one has  $v_1 \rightarrow 2$ , whereas the group velocities are vanishing in the other string sectors. At  $\Delta = 1$ ,  $v_1$  is different from the low-energy spin-wave velocity  $v_{sw} = \pi/2$  (shown as horizontal dotted line in Fig. 7).

## TWO DISJOINT INTERVALS

In this section we investigate the entanglement of two disjoint spin blocks after a quench. This is motivated by some recent holographic results, which also apply to irrational 1+1



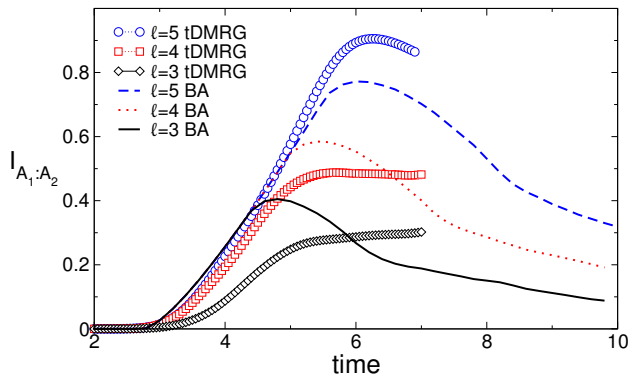


FIG. 8. Mutual information  $I_{A_1:A_2}$  between the two intervals  $A_1$  and  $A_2$  after the quench from the Néel state in the open  $XXZ$  chain. Here  $A_1$  and  $A_2$  are at the two edges of the chain and are of equal length  $\ell$ . The distance between  $A_1$  and  $A_2$  is  $d = 10$  lattice sites. The symbols are tDMRG results for  $\ell = 3, 4, 5$ . All the data are for  $\Delta = 2$ . The lines are the analytical results using the quasiparticle picture (22).

CFT (see e.g. Refs.[64, 67, 105–107]), that are in contrast with the quasiparticle picture. We focus on the behavior of the von Neumann mutual information  $I_{A_1:A_2}$  after a global quench. We consider the tripartition of the chain as  $A_1 \cup A_2 \cup B$ , where  $A_1$  and  $A_2$  are two disjoint intervals of equal length  $\ell$  and at distance  $d$ , while  $B$  is the remainder of the chain. The mutual information  $I_{A_1:A_2}$  is defined as

$$I_{A_1:A_2} \equiv S_{A_1} + S_{A_2} - S_{A_1 \cup A_2}, \quad (20)$$

with  $S_{A_{1(2)}}$  and  $S_{A_1 \cup A_2}$  being the entanglement entropies of  $A_{1(2)}$  and  $A_1 \cup A_2$ , respectively.

For an infinite system and two intervals of length  $\ell$  at a distance  $d$ , it is straightforward to derive the contribution to the mutual information of each quasiparticle with velocity  $v$ , namely [50]

$$I_{A_1:A_2} \propto -2 \max((d + \ell)/2, vt) + \max(d/2, vt) + \max((d + 2\ell)/2, vt), \quad (21)$$

which predicts  $I_{A_1:A_2} = 0$  for  $vt \leq d/2$ , a linear increase for  $d/2 < vt \leq (d + \ell)/2$ , followed by a linear decrease up to  $vt = (d + 2\ell)/2$ . In stark contrast, it has been suggested that the quasiparticle picture for the entanglement propagation does not hold in holographic contexts. The scenario of Ref. [107] predicts  $I_{A_1:A_2} = 0$  at any time: the idea is that quasiparticles originated at the same point in space and travelling one in  $A_1$  and the other in  $A_2$  do not remain maximally entangled when they are far apart from each other (a phenomenon known as scrambling).

To clarify whether the quasiparticle picture applies to interacting integrable models, here we discuss the behavior of  $I_{A_1:A_2}$  after the quench from the Néel state  $|\uparrow\downarrow\uparrow\downarrow\cdots\rangle$  in the  $XXZ$  chain. We restrict ourselves to the open  $XXZ$  spin chain. We always consider the situation with the two intervals  $A_1$  and  $A_2$  at the opposite edges of the chain, as it is convenient for the numerical simulations. This implies  $L = 2\ell + d$ .

In this case, the contribution of each quasiparticle is given by (21) with the replacement  $\ell \rightarrow 2\ell$ , but the formula is valid only before the revival time  $t_{\text{rev}} = L/v$ . Similar to (2), the final quasiparticle prediction for the mutual information is obtained by summing (and integrating) the contribution of all quasiparticles, i.e.

$$I_{A_1:A_2} = \sum_n \int d\lambda s_n(\lambda) \left[ -2 \max((d + 2\ell)/2, v_n(\lambda)t) + \max(d/2, v_n(\lambda)t) + \max((d + 4\ell)/2, v_n(\lambda)t) \right], \quad (22)$$

which, again, it is valid before the revival time, i.e. for  $t$  such that  $v_M t < L$ . In the following we compare (22) with tDMRG results.

It is well known that extracting the entanglement entropy of multiple disjoint intervals in DMRG simulations is a formidable task, in contrast with the single-interval entropy. Specifically, given the MPS representation of the state, the computational cost scales as  $\chi^6$  for the multi-interval, whereas it is only  $\chi^3$  for the single interval, with  $\chi$  the bond dimension of the MPS. This issue is even more dramatic out of equilibrium, where  $\chi$  grows exponentially with time. For this reason we can provide reliable data for  $I_{A_1:A_2}$  only for very small intervals, and up to short times after the quench.

Our results are presented in Figure 8. The symbols are the tDMRG data for  $I_{A_1:A_2}$  plotted as a function of the time after the quench. We show the data for  $\ell = 3, 4, 5$ , which are the only sizes we can simulate reliably, and only for  $t \lesssim 7$ . In our simulations, for all values of  $\ell$ , the two intervals are at fixed distance  $d = 10$ . The lines in the Figure are the analytic results obtained using (22). Clearly, the system sizes and time scales accessible in our tDMRG simulations do not allow us to reach a quantitative conclusion on the validity of (22) for the mutual information. Anyhow, we observe that the DMRG data are in a good overall qualitative agreement with the quasiparticle predictions (22). Indeed, the mutual information is zero for  $t < d/(2v_M)$ , then it starts growing (seemingly) linearly with time, up to a maximum value which is clearly visible for  $\ell = 5$  (but not for smaller  $\ell$ ). The few results available in the literature for the mutual information of two disjoint intervals for free systems [55, 108] show very similar effects when the lengths of the subsystems are very small as in our simulations. Hence, these DMRG results provide a strong support for the validity of the quasiparticle picture for  $I_{A_1:A_2}$ , signaling the absence of scrambling which takes place for CFTs with large central charge [107].